Inorg. Chem. **2008**, *47*, 5377−5385

Metathesis of Nitrogen Atoms within Triple Bonds Involving Carbon, Tungsten, and Molybdenum

Beth A. Burroughs, Bruce E. Bursten,* Shentan Chen, Malcolm H. Chisholm,* and Andy R. Kidwell

Department of Chemistry, The Ohio State University, 100 West 18th Avenue, Columbus, Ohio 43210

Received February 29, 2008

$(Bu^tO)_3Mo{\equiv}N$ and $W_2(OBu^t)_6(M{\equiv}M)$ react in hydrocarbons to form $Mo_2(OBu^t)_6(M{\equiv}M)$ and $(Bu^tO)_3W{\equiv}N$ via the reactive intermediate $MoW(OBu^t)_6(M{\equiv}M)$. $(Bu^tO)_3W{\equiv}N$ and $CH_3C{\equiv}N^{15}$ react in tetrahydrofuran (THF) at room temperature to give an equilibrium mixture involving $(Bu^tO)_3W{\equiv}N^{15}$ and $CH_3C{\equiv}N$. The $(Bu^tO)_3W{\equiv}N$ compound is similarly shown to act as a catalyst for N^{15}-atom scrambling between $MeC^{13}{\equiv}N^{15}$ and $PhC{\equiv}N$ to give a mixture of $MeC^{13}{\equiv}N$ and $PhC{\equiv}N^{15}$. From studies of degenerate scrambling of N atoms involving $(Bu^tO)_3W{\equiv}N$ and $MeC^{13}{\equiv}N$ in THF-d_8 by $^{13}C\{^1H\}$ NMR spectroscopy, the reaction was found to be first order in acetonitrile and the activation parameters were estimated to be $\Delta H^{\ddagger} = 13.4(7)$ kcal/mol and $\Delta S^{\ddagger} = -32(2)$ eu. A similar reaction is observed for $(Bu^tO)_3Mo{\equiv}N$ and $CH_3C{\equiv}N^{15}$ upon heating in THF-d_8. The reaction is suppressed in pyridine solutions and not observed for the dimeric $[(Bu^tMe_2SiO)_3W{\equiv}N]_2$. The reaction pathway has been investigated by calculations employing density functional theory on the model compounds $(MeO)_3M{\equiv}N$ and $CH_3C{\equiv}N$ where M = Mo and W. The transition state was found to involve a product of the 2 + 2 cycloaddition of M≡N and C≡N, a planar metalladiazacyclobutadiene. This resembles the pathway calculated for alkyne metathesis involving $(MeO)_3W{\equiv}CMe$, which modeled the metathesis of $(Bu^tO)_3W{\equiv}CBu^t$. The calculations also predict that the energy of the transition state is notably higher for M = Mo relative to M = W.

Introduction

The evolution of olefin metathesis involving transition-metal alkylidenes is one of the most fascinating and preparatively useful stories in chemistry.[1] Not long after the initial industrial discovery of olefin metathesis, Pennella et al.[2] disclosed a seemingly even more miraculous tale of triple-bond metathesis involving alkynes. In 1975, Katz and McGinnis[3] addressed the mechanism of olefin metathesis involving metal carbene intermediates and proposed that alkyne metathesis proceeded via a similar mechanism involving the 2 + 2 cycloaddition of C≡C and M≡C bonds to give a planar metallacyclobutadiene intermediate. This was soon thereafter demonstrated by the elegant work of Schrock and co-workers[4] involving the reactions between tungsten trialkoxyalkylidynes and -alkynes. This reaction too has entered into the tool kit of organic reagents.[5] We describe here our findings of the metathesis reaction involving M−N and C−N triple bonds where the metals are either W or Mo. A preliminary report on this work appeared in 2003,[6] and subsequently related work was reported by Johnson in 2005.[7,8]

Results and Discussion

$Mo{\equiv}N + W{\equiv}W \rightarrow Mo{\equiv}W + W{\equiv}N$. The reaction between $(Bu^tO)_3Mo{\equiv}N$[9] and $(Bu^tO)_3W{\equiv}W(OBu^t)_3$[10] proceeds quite rapidly in hydrocarbon solutions to give the

* To whom correspondence should be addressed. E-mail: chisholm@chemistry.ohio-state.edu.

(1) (a) Grubbs, R. H. *Adv. Synth. Catal.* **2007**, *349*, 34. (b) Bielawski, C. W.; Grubbs, R. H. *Prog. Polym. Sci.* **2007**, *32*, 1. (c) Grubbs, R. H. *Prix Nobel* **2006**, 194. (d) Schrock, R. R.; Czekelius, C. *Adv. Synth. Catal.* **2007**, *349*, 55. (e) Schrock, R. R. *Adv. Synth. Catal.* **2007**, *349*, 41. (f) Schrock, R. R. *Prix Nobel* **2006**, 216.
(2) Pennella, F.; Banks, R. L.; Bailey, G. C. *Chem. Commun.* **1968**, 1548.
(3) Katz, T. J.; McGinnis, J. *J. Am. Chem. Soc.* **1975**, *97*, 1592.
(4) Wengrovius, J. H.; Sancho, J.; Schrock, R. R. *J. Am. Chem. Soc.* **1981**, *103*, 3932.
(5) Schrock, R. R. *Chem. Rev.* **2002**, *102*, 145.
(6) Chisholm, M. H.; Delbridge, E. E.; Kidwell, A. R.; Quinlan, K. R. *Chem. Commun.* **2003**, 126.
(7) Gdula, R. L.; Johnson, M. J. A.; Ockwig, N. W. *Inorg. Chem.* **2005**, *44*, 9140.
(8) Gdula, R. L.; Johnson, M. J. A. *J. Am. Chem. Soc.* **2006**, *128*, 9614.
(9) Chan, D. M.-T.; Chisholm, M. H.; Folting, K.; Huffman, J. C.; Marchant, N. S. *Inorg. Chem.* **1986**, *25*, 4170.

10.1021/ic8003917 CCC: $40.75
Published on Web 05/06/2008

mixed-metal MoW triply bonded complex $MoW(OBu^t)_6$ with the formation of $(Bu^tO)_3W{\equiv}N$.[11] The compound $MoW(OBu^t)_6$ can readily be identified in the mass spectrum by the presence of a molecular ion that shows the distinct isotopic distribution predicted for a MoW-containing species. It is also seen in the ^1H NMR spectrum where two Bu^t singlets are observed, as is expected for each of the three alkoxide ligands bound to each metal. However, it has not been possible to isolate this heteronuclear MM′-bonded compound because this compound reacts further with $(Bu^tO)_3Mo{\equiv}N$ with the ultimate formation of $Mo_2(OBu^t)_6$ and $(Bu^tO)_3W{\equiv}N$. The compounds $Mo_2(OBu^t)_6$, $MoW(OBu^t)_6$, and $W_2(OBu^t)_6$ show similar solubilities and almost certainly cocrystallize. The driving force for this reaction rests with the favorable redox reaction involving the two metals, $Mo^{VI} + W^{III} \rightarrow Mo^{III} + W^{VI}$, and almost certainly proceeds by way of an activated trinuclear cluster involving a triply bridging nitride. Structural precedent for this exists in the form of the tetranuclear cluster $Mo_4(\mu_3\text{-}N)_2(OPr^i)_{12}$[12] and in related $M_3(\mu_3\text{-}O)(OR)_{10}$,[13] $MoW_2(\mu_3\text{-}O)(OR)_{10}$,[13] and $W_3(\mu_3\text{-}P)(OR)_9$ clusters.[14]

Alkylidyne and Nitride Ligand Transfer between Molybdenum and Tungsten. Although the triple bonds between the metals Mo and W and between C and N are estimated to be ~120−155 kcal/mol,[15,16] they are kinetically labile and readily transferable between metal centers as shown in reactions 1–3, where L = Bu^tO.

$$L_3W{\equiv}{}^{13}CMe + L_3Mo{\equiv}CPh \rightleftharpoons L_3W{\equiv}CPh + L_3Mo{\equiv}{}^{13}CMe \quad (1)$$

$$L_3W{\equiv}{}^{13}CMe + L_3Mo{\equiv}N \rightleftharpoons L_3W{\equiv}N + L_3Mo{\equiv}{}^{13}CMe \quad (2)$$

$$L_3W{\equiv}{}^{15}N + L_3Mo{\equiv}N \rightleftharpoons L_3W{\equiv}N + L_3Mo{\equiv}{}^{15}N \quad (3)$$

These reactions can be monitored by NMR spectroscopy in solvents such as toluene-d_8. The presence of ^{183}W, $I = {}^1/_2$, which occurs in ~15% natural abundance aids in the detection of ^{13}C and ^{15}N nuclei by the presence of $^1J_{^{183}W}$ satellites.

These observations led us to interrogate the metathesis reactions involving M≡N and C≡N described below.

$$W{\equiv}N^* + RC{\equiv}N \rightleftharpoons W{\equiv}N + RC{\equiv}N^*$$

The compound $(Bu^tO)_3W{\equiv}{}^{15}N$ is readily prepared from the reaction between $W_2(OBu^t)_6$ and labeled acetonitrile $CH_3C{\equiv}{}^{15}N$, and if this reaction is carried out in a hydrocarbon solvent, the tungsten nitride is formed as a finely divided microcrystalline product.[17] The compound $(Bu^tO)_3W{\equiv}N$ is only sparingly soluble in solvents such as toluene and in the solid state exists as an infinite polymeric chain involving connectivity (→ W≡N → W≡N →).[11] Because of poor solubility in hydrocarbons, our studies of N-atom exchange were carried out in the more polar and coordinating solvent tetrahydrofuran (THF). The molybdenum analogue $(Bu^tO)_3Mo{\equiv}N$ adopts an analogous structure in the solid state but is somewhat more soluble in hydrocarbon solvents because of the weaker donor strength of the less polar Mo≡N bond.

The reaction between $MeC{\equiv}{}^{15}N$ and $(Bu^tO)_3W{\equiv}N$ in THF-d_8 was followed by ^{15}N NMR. The signal at $\delta \sim 248$ ppm decreased in intensity as the signal due to $(Bu^tO)_3W{\equiv}{}^{15}N$ grew in intensity at $\delta \sim 732$ ppm. A similar reaction was carried out employing $(Bu^tO)_3Mo{\equiv}N$ in THF-d_8, but no reaction was observed at room temperature. However, heating the solution to 70 °C did bring about a similar reaction with the formation of $(Bu^tO)_3Mo{\equiv}{}^{15}N$.

The tungsten nitride complex was then used as a catalyst for the N-atom exchange as shown in reaction 4. The reactions were again monitored by ^{15}N NMR spectroscopy.

$$MeC{\equiv}{}^{15}N + RC{\equiv}N \overset{\text{cat.}}{\rightleftharpoons} MeC{\equiv}N + RC{\equiv}{}^{15}N \quad (4)$$

A broad range of nitriles was chosen both to test the generality of the N-atom exchange and to test the tolerance of $(Bu^tO)_3W{\equiv}N$ toward various functional groups. For the groups where R = ortho and p-C_6H_4F, $-C_6H_4Cl$, $(CH_2)_4Cl$, Me_3C, Ph, $PhCH_2$, Ph_2CH, Ph_3C, and $-CH{=}CHCN$ scrambling of the label was observed. The reaction is quite tolerant to steric factors and carbon−halogen as well as C=C bonds. Rather interestingly, the o-fluorophenyl nitrile showed $^{15}N-{}^{19}F$ coupling, with its signal at $\delta = 271.7$ ppm appearing as a doublet (see Figure 1). At this point, it is worth noting that Johnson has recently demonstrated that alkynes will react with fluorinated alkoxide molybdenum and tungsten nitrides to yield the respective alkylidynes and nitriles.[8]

In order to establish that in reaction 4 the metathesis involved solely N-atom exchange and not a cyano group exchange, we also examined the reaction between $Me^{13}C{=}N$, $MeC{\equiv}{}^{15}N$, and PhC≡N. As shown in Figure 2, the exchange catalyzed by $(Bu^tO)_3W{\equiv}N$ involved exclusively W≡N and C≡N metathesis.

The exchange reactions noted above do not occur in pyridine-d_5, which is a good donor to tungsten and presumably blocks coordination of the weaker nitrile donor. Also the siloxide-bridged dimeric compound $[(Bu^tMe_2SiO)_3W{\equiv}N]_2$[18] does not react with $MeC{\equiv}{}^{15}N$.

(10) (a) Chisholm, M. H.; Extine, M. W. *J. Am. Chem. Soc.* **1975**, *97*, 5625. (b) Chisholm, M. H.; Gallucci, J. C.; Hollandsworth, C. B. *Polyhedron* **2006**, *25*, 827.

(11) Chisholm, M. H.; Hoffman, D. M.; Huffman, J. C. *Inorg. Chem.* **1983**, *22*, 2903.

(12) Chisholm, M. H.; Folting, K.; Huffman, J. C.; Leonelli, J.; Marchant, N. S.; Smith, C. A.; Taylor, L. C. E. *J. Am. Chem. Soc.* **1985**, *107*, 3722.

(13) Chisholm, M. H.; Folting, K.; Huffman, J. C.; Kober, E. M. *Inorg. Chem.* **1985**, *24*, 241.

(14) Chisholm, M. H.; Folting, K.; Pasterczyk, J. W. *Inorg. Chem.* **1988**, *27*, 3057.

(15) Chisholm, M. H.; Davidson, E. R.; Quinlan, K. B. *J. Am. Chem. Soc.* **2002**, *124*, 15351.

(16) Cherry, J.-P. F.; Johnson, A. R.; Baraldo, L. M.; Tsai, Y.-C.; Cummins, C. C.; Kryatov, S. V.; Rybak-Akimova, E. V.; Capps, K. B.; Hoff, C. D.; Harr, C. M.; Nolan, S. P. *J. Am. Chem. Soc.* **2001**, *123*, 7271.

(17) Weingrovius, J. H.; Sancho, J.; Schrock, R. R. *J. Am. Chem. Soc.* **1981**, *103*, 3932.

(18) Chisholm, M. H.; Folting, K.; Lynn, M. L.; Tiedtke, D. B.; Lemiogno, F.; Eisenstein, O. *Chem.−Eur. J.* **1999**, *5*, 2318.

(19) Parkin, I. P.; Folting, K. *J. Chem. Soc., Dalton Trans.* **1992**, 2343.

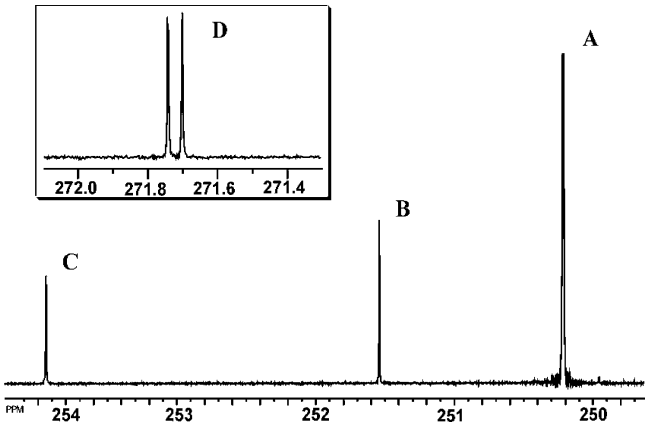

Figure 1. ^{15}N NMR spectra of $Cl(CH_2)_4C{\equiv}{}^{15}N$ (**B**), *p*-$Cl(C_6H_4)C{\equiv}{}^{15}N$ (**C**), and *o*-$F(C_6H_4)C{\equiv}{}^{15}N$ (**D**), byproducts of a scrambling reaction with $(^tBuO)_3W{\equiv}N$ and $MeC{\equiv}{}^{15}N$ (**A**).

The chiral menthoxide complexes, both [(+)-men-O]$_3$W≡N[19] and [(−)-men-O]$_3$W≡N[19], were prepared and shown to catalyze exchange of N between MeC≡^{15}N and the bulky enantiomerically pure (*S*)-2-(6-methoxy-2-napthyl)propionitrile (see reaction 5). This raises the possibility of enantioselective N-atom exchange, but we have not investigated this further at this time.

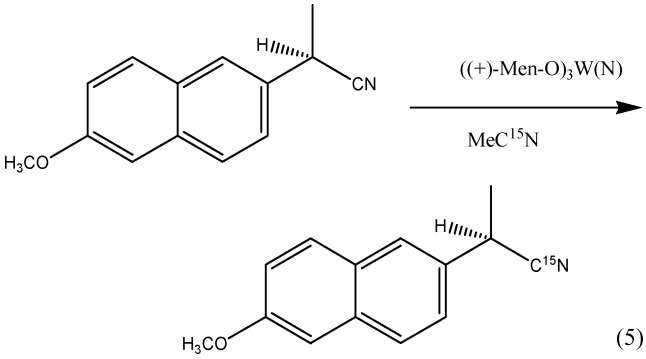

(5)

Estimation of Activation Parameters. The atom exchange reaction proceeds at convenient rates under ambient conditions to allow its study by a variety of conventional techniques. However, the specifics of the system proved problematic. For example, the limited solubility and the high air sensitivity of $(Bu^tO)_3W{\equiv}N$ made following the course of the reaction by react-IR unreliable. Similarly, mass spectrometry was complicated by relative intensities of RCN^+ and $RCNH^+$ ions due to experimental conditions, and ^{15}N NMR required too long acquisition times. We finally resorted to the use of ^{13}C NMR spectroscopy to follow the reaction between $Me^{13}C{\equiv}N$ and $(Bu^tO)_3W{\equiv}{}^{15}N$. The ^{13}C NMR signal for $Me^{13}C{\equiv}N$ appears as a singlet at $\delta = 116.96$ ppm and upon ^{15}N-atom exchange coupling to ^{15}N, $I = {}^1/_2$, leads to a doublet at $\delta = 117.01$ and 116.77 ppm. The line-shape analysis program in XWIN-NMR makes it possible to extrapolate relative concentrations of $Me^{13}C{\equiv}N$ and $Me^{13}C{\equiv}{}^{15}N$ with time and, hence, obtain data for kinetics. By keeping the concentration of $(Bu^tO)_3W{\equiv}{}^{15}N$ constant and varying the concentration of nitrile, it was determined that the reaction is first order in nitrile (see the Experimental Section). A variable-temperature study (20−50 °C) following the decay of $Me^{13}C{\equiv}N$ allowed for the production of the Eyring plot shown in Figure 3. Based on this, an estimation of the activation parameters can be made: $\Delta H^{\ddagger} = +13.4(7)$ kcal/mol and $\Delta S^{\ddagger} = -32(2)$ eu.

Although the alkyne metathesis reaction has been well explored in terms of its synthetic utility and reaction pathway, to our knowledge, the kinetics and activation parameters have only been determined for a related reaction involving the exchange of alkyne units and the metallacyclobutadiene complex, $(DIPP)_3W(C_3R_3)$, where R = Et and Pr^n and DIPP = 2,6-diisopropyl phenoxide, with 3-hexyne-d_{10}[20] (see reaction 6, where R = Et and Pr^n and R′ = CD_2CD_3).

$$(DIPP)_3W(C_3R_3) + R'C{\equiv}CR' \rightarrow (DIPP)_3W(C_3RR'_2) + RC{\equiv}CR \quad (6)$$

For R = Et, a variable-temperature study led to the determination of $\Delta H^{\ddagger} = +26.1(4)$ kcal/mol and $\Delta S^{\ddagger} = +15.2(15)$ eu, while for R = Pr^n, $\Delta H^{\ddagger} = +25.4(5)$ kcal/mol and $\Delta S^{\ddagger} = +16.3(16)$ eu.[20] The reaction was also shown to be first order in tungsten and independent of 3-hexyne-d_{10} in the concentration range studied. Thus, the activation parameters reported by Schrock and co-workers pertain to a rate-limiting elimination of RC≡CR from the metallacyclobutadiene, whereas in our study, the parameters most likely reflect an associative 2 + 2 reaction. Qualitatively, we can see that this is reflected in the positive entropy of activation for reaction 6 and the negative $\Delta S^{\ddagger}$ value for the N-atom metathesis reaction.

Theoretical and Computational Considerations. Following the initial theoretical considerations of Bursten[21] in 1983, considerable attention has been given to the relative stabilities and bonding in metallacyclobutadiene and metallatetrahedrane complexes and their role in the alkyne metathesis reaction.[22–24] This work has led up to the most recent 2006 publication[25] dealing with the total reaction pathway for alkyne metathesis by molybdenum and tungsten $(RO)_3M{\equiv}CMe$ complexes as determined by density functional theory employing B3LYP and the effective core potentials of Hay and Walt with a double-ζ valence basis set including one f polarization function for Mo and W atoms.

We have employed density functional theory using exchange and gradient-corrected correlation functional PW91 to investigate the reaction pathway leading to the N-atom metathesis reactions described above. Two kinds of basis set systems, BS-I (LanL2DZ basis sets augmented by an f polarization function for metal atoms and the 6-31G* basis sets for nonmetal atoms) and BS-II (SDD basis sets for metal atoms and cc-pVTZ basis sets for nonmetal atoms), were used to study the potential energy surfaces of the metathesis reactions between $(MeO)_3M{\equiv}N$ (where M = W, Mo) and MeC≡N. The reaction pathways found by employing a larger basis set system, BS-II, are similar to those found by using

(20) Chirchill, M. R.; Ziller, J. W.; Freudenberger, J. H.; Schrock, R. R. *Organometallics* **1984**, *3*, 1554.
(21) Bursten, B. E. *J. Am. Chem. Soc.* **1983**, *105*, 121.
(22) Woo, J.; Folga, E.; Ziegler, T. *Organometallics* **1993**, *12*, 1289.
(23) Lin, Z.; Hall, M. B. *Organometallics* **1994**, *12*, 2878.
(24) Sheng, Y.-H.; Wu, Y.-D. *J. Am. Chem. Soc.* **2001**, *123*, 6662.
(25) Guochen, J. Z.; Lin, Z. *Organometallics* **2006**, *25*, 1812.

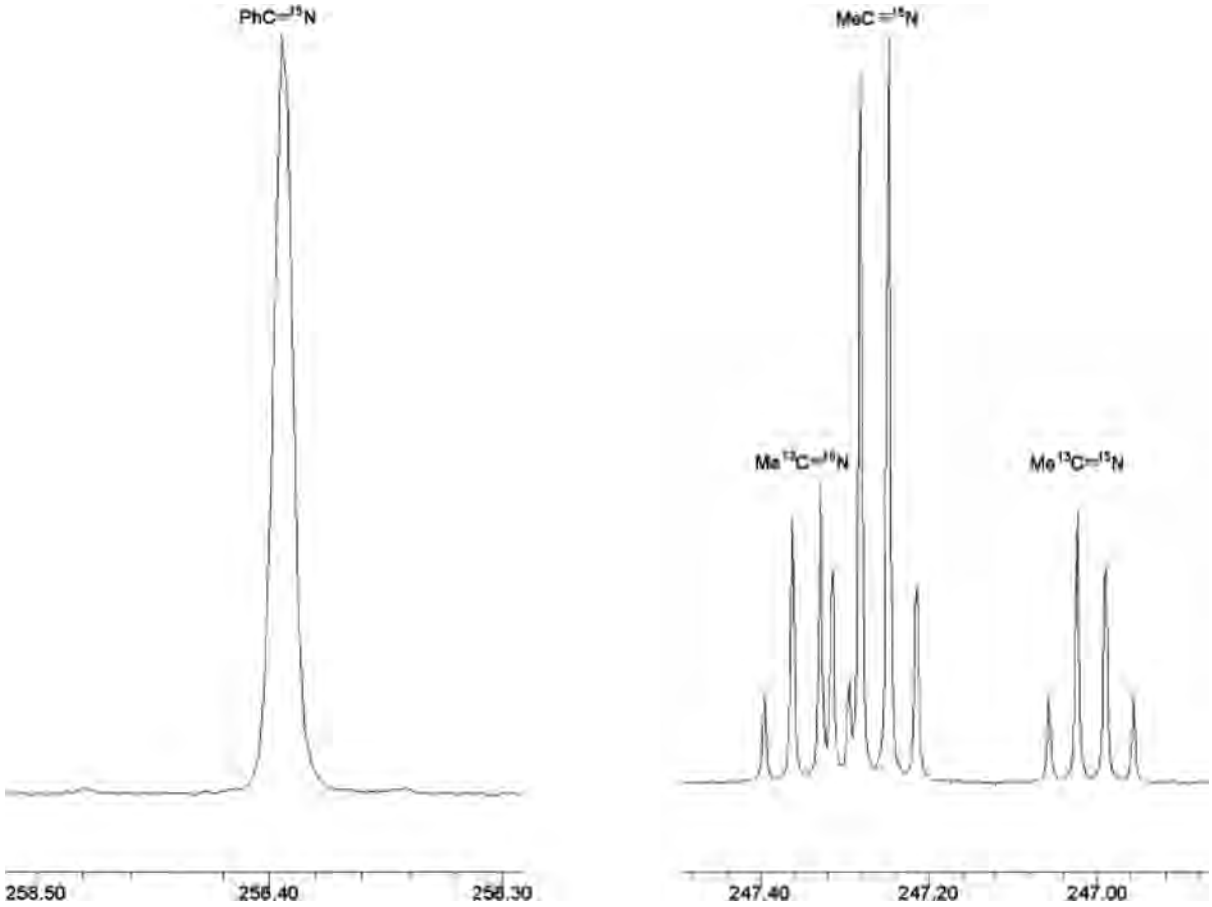

Figure 2. ^{15}N NMR spectra of the reaction between Me^{13}C≡N, MeC≡^{15}N, and PhC≡N in the presence of a trace of (^{t}BuO)$_3$W≡N recorded in THF-d_8 at 298 K, 50.6 MHz. The PhC≡^{15}N signal shows enhancement due to ^{15}N-atom exchange and appears as a singlet due to lack of coupling to ^{1}H or ^{13}C, whereas the MeC≡N ^{15}N signal shows coupling to ^{1}H, $^{3}J^{1}\mathrm{H}-^{15}N = 1.7$ Hz, and for Me^{13}C≡^{15}N coupling to ^{13}C, $^{1}J^{13}\mathrm{C}-^{15}N = 17$ Hz. The signal thus appears as a central 1:3:3:1 quartet flanked by ^{13}C satellites. The unsymmetrical nature of the ^{13}C satellites arises from ^{12}C/^{13}C isotopic chemical shift perturbation.

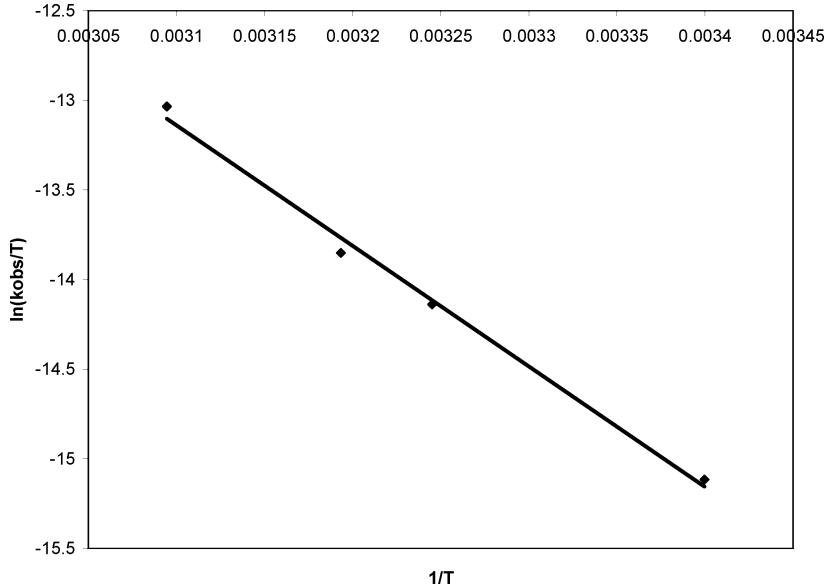

Figure 3. Eyring plot of $\ln(k_{obs}/T)$ vs $1/T$ where $y = -6727x + 7.7142$ and $R^2 = 0.9937$. The enthalpy parameters were calculated to be $\Delta H^{\ddagger} = +13.4(7)$ kcal/mol and $\Delta S^{\ddagger} = -32(2)$ eu for the ^{15}N isotope exchange reaction between (^{t}BuO)$_3$W^{15}N and Me^{13}CN.

BS-I. For both basis set systems, the same number of stationary points with similar structures on the reaction pathway was found for each reaction. The slightly higher activation free energies obtained by using BS-II than by using BS-I are mainly due to the lack of an f polarization function for metal atoms in BS-II. This is evident by comparing the activation free energies for the reaction between (MeO)$_3$W≡N and MeC≡N obtained from BS-I, BS-II, BS-III (LanL2DZ for metal atoms and 6-31G* for nonmetal atoms), and BS-IV (SDD for metal atoms and 6-31G* for

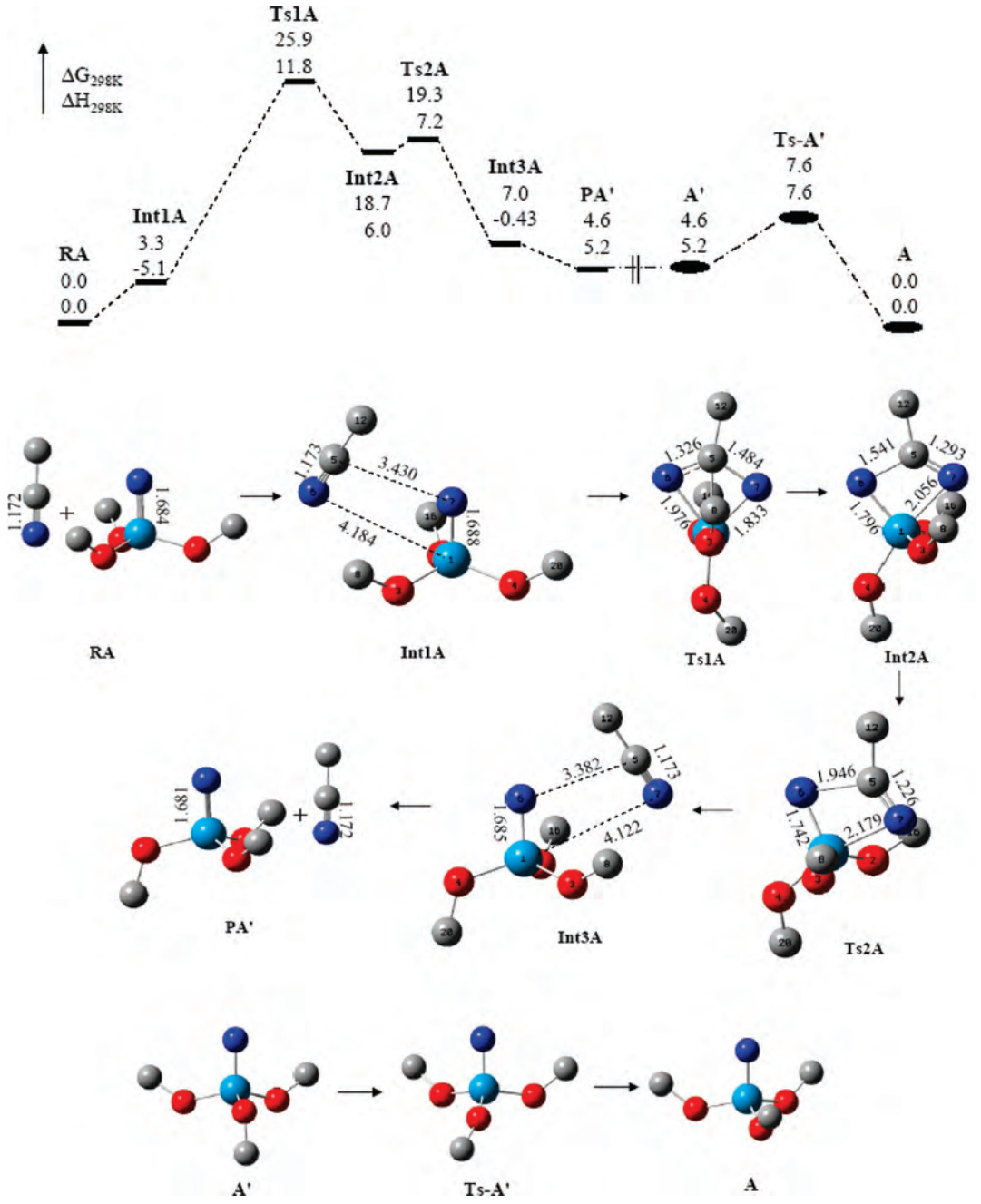

Figure 4. Free energy (at 298 K) profiles for the N-atom exchange reaction between $(MeO)_3W{\equiv}N$ and $MeC{\equiv}N$ and structures of transition states and intermediates with selected calculated structural parameters (Å).

nonmetal atoms). The activation free energy is defined by the difference of free energies between the high-lying transition structure (TS1A) and the starting materials. The calculated activation free energies from BS-I to BS-IV are 25.9, 31.7, 29.4, and 29.3 kcal/mol, respectively. The almost same values based on BS-III and BS-IV indicate that the different effective core potentials seem to have no effect on the activation free energy for this calculation. Employment of an the f function brings down the energy by about 3.5 kcal/mol, while employment of the triple basis sets cc-pVTZ for nonmetal atoms slightly increases the activation free energy but does not have a significant effect on the reaction pathway. The calculated activation free energy by using BS-I is closest to the experimental value. On the basis of the above facts, we presented our results calculated by using BS-I.

The calculated free energy profiles for the N-atom exchange reaction between $(MeO)_3M{\equiv}N$ and $MeC{\equiv}N$ and structures of transition states and intermediates with selected calculated structural parameters (Å) for W and Mo using BS-I are shown in Figures 4 and 5, respectively.

The overall reaction between $(MeO)_3W{\equiv}N$ and $MeC{\equiv}N$ involves N-atom exchange and a conformation change. The N-atom exchange is endothermic ($\Delta G = 4.6$ kcal/mol, which is principally caused by the presence of the different conformations of $(MeO)_3W{\equiv}N$ in RA and PA′). In this step,

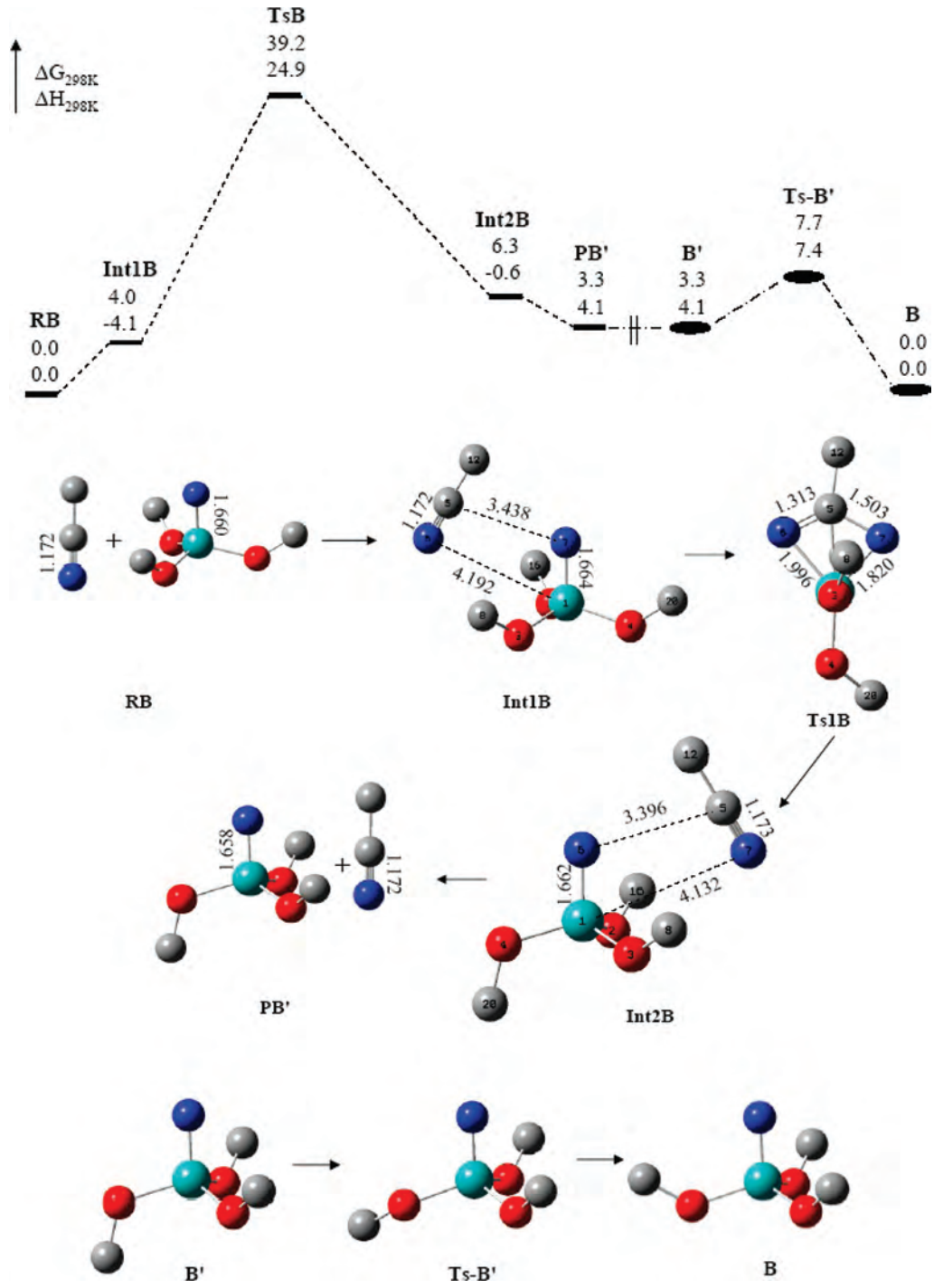

Figure 5. Free energy (at 298 K) profiles for the N-atom exchange reaction between $(MeO)_3Mo{\equiv}N$ and $MeC{\equiv}N$ and structures of transition states and intermediates with selected calculated structural parameters (Å).

two transition states, Ts1A and Ts2A, are located. The higher-lying transition state Ts1A connects minima Int1A and Int2A. The intermediate Int2A is transformed into another intermediate Int3A through transition state Ts2A. However, we shall not overemphasize the existence of intermediate Int2A and Ts2A because the barrier for transformation from Int2A to Int3A is only about 0.6 kcal/mol and the analogous intermediate and transition state were not found in the reaction pathway involving the molybdenum analogue. Dissociation of Int1A and Int3A, leading to the formation of separate tungsten nitride and acetonitrile, can occur without barriers. Int1A has a free energy of 3.3 kcal/mol, which is essentially caused by the loss of entropy associated with the interaction between $(MeO)_3W{\equiv}N$ and $MeC{\equiv}N$. The higher free energy of Int3A than that of PA′ is also caused by such a loss of entropy. As can be seen in Figure 4, different conformations of $(MeO)_3W{\equiv}N$ are present in the product of the N-atom exchange step, PA′, and the reactant, RA. The conformer A′ in PA′ is calculated to be higher in free energy than conformer A in RA by 4.6 kcal/mol, which accounts for the difference of the free energies between RA and PA′. A′ can be readily transformed into

the more stable conformer A by crossing an energy barrier of about 3 kcal/mol. A similar metathesis pathway was calculated for the reaction between $(MeO)_3Mo{\equiv}N$ and $MeC{\equiv}N$ except that neither the analogue of Int2A nor the analogue of TS2A was found in this pathway. The transition state Ts1B connects minima Int1B and Int2B and further dissociates to form $(MeO)_3Mo{\equiv}N$ and $MeC{\equiv}N$. Similar conformation transfer from B′ to B was also observed.

The transition state Ts1A was calculated to be higher in free energy than the starting materials by 25.9 kcal/mol (about 12 kcal/mol in enthalpy). This calculated free-energy barrier for the N-atom exchange reaction between $(MeO)_3W{\equiv}N$ and $MeC{\equiv}N$ is in good agreement with the experimental observations, while for the reaction involving $(MeO)_3Mo{\equiv}N$ and $MeC{\equiv}N$, the transition state Ts1B was calculated to be higher in free energy than the starting materials by 39.2 kcal/mol, which is about 13 kcal/mol higher than that for the tungsten analogue. This result is also consistent with the experimental observation that N-atom exchange between $(Bu^tO)_3Mo{\equiv}N$ and $MeC{\equiv}N$ only occurs at elevated temperatures.

The calculated pathways leading to N-atom metathesis and alkyne metathesis bear the similarity that reactions proceed through 2 + 2 cycloaddition but that differences exist between them. In both types of metathesis reactions, the ring-closing step is the rate-determining step. However, no metal alkyne adduct can be located along the pathway for alkyne metathesis, and this was attributed to the fact that the d^0 metal center cannot stabilize an alkyne complex by back-donation. Metal nitrile complexes (i.e., Int1A and Int1B) were found along the reaction coordinates for the N-atom exchange reactions, and the formation of metal nitrile complexes is probably due to the dipole−dipole interactions and weak van der Waals interactions between the metal nitride fragment and nitrile because the distance between the two fragments is fairly large and both fragments are almost unperturbed. Density functional theory may have a problem handling such interactions, and a higher level of theoretical considerations might be needed to study these weakly associated complexes.

Concluding Remarks

The facility of N-atom metathesis described herein together with the recent report by Johnson et al.[7,8] on the metathesis involving Mo≡N bonds and alkynes to form molybdenum alkylidynes and organic nitriles shows the kinetic lability of these strong M≡N bonds. If these reactions can be coupled to Cummins and co-workers'[26–29] reductive cleavage of N≡N by $Mo(NR_2)_3$ compounds, then a relatively simple and inexpensive route to ^{15}N-labeled organic compounds will be achieved. Interestingly, the compound $(^tBuO)_3CrN$[30] does not appear to entertain this type of chemistry, though in reactions with $M_2(O^tBu)_6$, redox chemistry is observed with the formation of the blue volatile compound $Cr(O^tBu)_4$[31] along with the compounds $(^tBuO)_3MN$ as identified by their molecular ions in the mass spectrometer.

Experimental Section

General Procedures. All operations were carried out under an inert atmosphere of argon with dry and deoxygenated solvents using standard Schlenk-line and drybox procedures. All chemicals were purchased from commercial sources and were used as received unless duly noted. Aromatic and aliphatic hydrocarbon solvents were dried over either sodium or potassium, and THF and diethyl ether were distilled from sodium benzophenone. CH_3CN was dried over CaH_2 and distilled prior to use. All distilled solvents were stored over 4 Å molecular sieves. The nitriles employed in the N-atom exchange reactions were stored over 4 Å sieves and were subjected to three freeze−thaw−degas cycles prior to use. Deuterated solvents and $^{13}C/^{15}N$-labeled isotopically enriched compounds were obtained from Cambridge Isotope Laboratories, Inc., and were similarly dried and degassed prior to use.

Syntheses. The compounds $W_2(OR)_6$, where R = OBu^t,[10] (+)-menthyl,[19] and (−)-menthyl[19] were prepared by alcoholysis reactions involving $W_2(NMe_2)_6$,[32] $(Bu^tO)_3CrN$,[30] $(Bu^tO)_3MoN$,[9] and $(Bu^tO)_3MoCPh$,[33] were prepared according to literature procedures.

Spectroscopic Methods. ^1H, ^{19}F, $^{13}C\{^1H\}$, and ^{15}N NMR spectra were recorded on Bruker Avance 400 and 500 MHz spectrometers. IR spectra were recorded on a Perkin-Elmer GX FT-IR spectrophotometer as KBr pellets. Mass spectra were recorded on a Kratos MS25 RFA double-focusing magnetic sector mass spectrometer as positive ions.

Computational Methods. All calculations were performed using density functional theory as implemented in the *Gaussian 03* suite of programs.[34] The PW91PW91[35] [Perdew and Wang's 1991 exchange and gradient-corrected correlation functional] density functional theory was used for all calculations. Two types of basis set systems, BS-I and BS-II were used for potential energy surface calculations. In BS-I, the LanL2DZ[36] basis sets augmented by an f polarization function [ζ(f) = 0.823, W; 1.043, Mo][37] were used for transition-metal atoms and the 6-31G* basis sets[38] were used for all other nonmetal atoms in the model compounds. In BS-II,

(26) Cummins, C. C. *Chem. Commun.* **1998**, 1778.
(27) Laplaza, C. E.; Johnson, M. J. A.; Peters, J.; Odom, A. L.; Kim, E.; Cummins, C. C.; George, G. N.; Pickering, I. J. *J. Am. Chem. Soc.* **1996**, *118*, 8623.
(28) Laplaza, C. E.; Johnson, A. R.; Cummins, C. C. *J. Am. Chem. Soc.* **1996**, *118*, 709.
(29) Laplaza, C. E.; Cummins, C. C. *Science (Washington, D.C.)* **1995**, *268*, 861.
(30) (a) Chiu, H.-T.; Chen, Y.-P.; Chuang, S.-H.; Jen, J.-S.; Lee, G.-H.; Peng, S.-M. *Chem. Commun.* **1996**, 139. (b) Fickes, M. G.; Davis, E. M.; Cummins, C. C. *J. Am. Chem. Soc.* **1995**, *117*, 6384.
(31) Alyea, E. C.; Basi, J. S.; Bradley, D. C. *J. Chem. Soc. A* **1971**, 772.
(32) Chisholm, M. H.; Cotton, F. A.; Extine, M. W.; Stultz, B. R. *J. Am. Chem. Soc.* **1976**, *98*, 4477.
(33) Strutz, H.; Schrock, R. R. *Organometallics* **1984**, *3*, 1600.
(34) Frisch, M. J.; Trucks, G. W.; Schlegel, H. B.; Scuseria, G. E.; Robb, M. A.; Cheeseman, J. R.; Montgomery, J. A.; Vreven, T., Jr.; Kudin, K. N.; Burant, J. C.; Millam, J. M.; Iyengar, S. S.; Tomasi, J.; Barone, V.; Mennucci, B.; Cossi, M.; Scalmani, G.; Rega, N.; Petersson, G. A.; Nakatsuji, H.; Hada, M.; Ehara, M.; Toyota, K.; Fukuda, R.; Hasegawa, J.; Ishida, M.; Nakajima, T.; Honda, Y.; Kitao, O.; Nakai, H.; Klene, M.; Li, X.; Knox, J. E.; Hratchian, H. P.; Cross, J. B.; Cammi, R.; Pomelli, C.; Ochterski, J. W.; Ayala, P. Y.; Morokuma, K.; Voth, G. A.; Salvador, P.; Dannenberg, J. J.; Zakrewski, V. G.; Dapprich, S.; Daniels, A. D.; Strain, M. C.; Farkas, O.; Malick, D. K.; Rabuck, A. D.; Raghavachari, K.; Fresman, J. B.; Ortiz, J. V.; Cui, Q.; Baboul, A. G.; Clifford, S.; Cioslowski, J.; Stefanov, B. B.; Liu, G.; Liashenko, A.; Piskorz, P.; Komaromi, I.; Martin, R. L.; Fox, D. J.; Keith, T.; Al-Laham, M. A.; Peng, C. Y.; Nanayakkara, A.; Challocombe, M.; Gill, P. M. W.; Johnson, B.; Chen, W.; Wong, M. W.; Gonzalez, C.; Pople, J. A. *Gaussian 03*, revision C.02;Gaussian, Inc.: Wallingford, CT, 2004.

the SDD basis sets[39] were used for transition-metal atoms and the cc-pVTZ basis sets[40] were used for all other nonmetal atoms. Two other basis set systems, BS-III (LanL2DZ for metal atoms and 6-31G* for nonmetal atoms) and BS-IV (SDD for metal atoms and 6-31G* for nonmetal atoms), were also used for activation energy calculations to assess the influences of different effective core potential and the f polarization functions. All of the structures were fully optimized. Frequency calculations were also performed to confirm that all of the stationary points were minima or transition states (no imaginary frequency for the minimum and one imaginary frequency for the transition state). Intrinsic reaction coordinate[41] calculations were carried out on transition states to confirm that these structures are indeed connecting two minima. The discussed energies are relative Gibbs free energies ($\Delta G_{298\ K}$). The relative enthalpies ($\Delta H_{298\ K}$) are also provided for reference. All of the relative energies were defined with respect to the starting materials.

Synthesis of $(O^tBu)_3W{\equiv}{}^{15}N$. $W_2(^tBuO)_6$ (1.00 g, 1.24 mmol) was dissolved in hexane (250 mL) with rapid stirring. A hexane solution (10 mL) containing $MeC^{15}N$ (0.4 g, 9.5 mmol) was added to the dark-red solution with rapid stirring. Immediately after the addition of acetonitrile, the color changed to dark amber and a brown precipitate was formed. The brown precipitate [$(^tBuO)_3W{\equiv}{}^{15}N$] was collected over an air-sensitive filter frit, washed with three 10 mL portions of hexane, and dried in vacuo (500 mg, 96% yield). ^{1}H NMR (500 MHz, THF-d_8): δ 1.49 (s, 9H, OC(CH_3)$_3$). ^{15}N NMR (500 MHz, THF-d_8): δ 732 [(s), $J(^{183}W-{}^{15}N)$ = 54 Hz]. IR (KBr plates, Nujol mull): 934 cm^{-1} [$\nu(W^{15}N)$]; the 1020 cm^{-1} band attributed to ν(WN) for the unlabeled derivative was absent.

Synthesis of [(+)-Men-O]$_3$W≡N. [(+)-Men-O]$_3$W≡CEt (500 mg, 0.72 mmol) was dissolved in hexane (150 mL) with rapid stirring. Benzonitrile (1 mL) was added via a gastight syringe to the stirring hexane solution. The vessel was placed under vacuum, sealed, and stirred for 24 h. After stirring, the volume was reduced to ca. 2 mL of hexane. Acetonitrile (5 mL) was added, and a brown jellylike solid was formed. The solid was titurated (15 min) until a brown powder formed. The brown solid was filtered, washed with acetonitrile five times, and dried in vacuo (389 mg, 81% yield). ^{1}H NMR (500 MHz, C_6D_6): δ 4.77 (m, 1H), 2.91 (d, 1H), 2.54 (m, 1H), 1.82 (d, 2H), 1.58 (qt, 2H), 1.34 (d, 3H), 1.19 and 1.15 (d of d, 8H), 1.0 (m, 1H). ^{13}C NMR (500 MHz, C_6D_6): δ 88.41, 51.59, 45.49, 35.12, 32.28, 25.87, 23.23, 23.13, 21.59, 16.45. IR (KBr plates, Nujol mull): 1023 cm^{-1} [ν(WN)].

Synthesis of [(−)-Men-O]$_3$W≡N. [(−)-Men-O]$_3$W≡CEt (750 mg, 1.09 mmol) was dissolved in hexane (150 mL) with rapid stirring. Benzonitrile (1 mL) was added via a gastight syringe to the stirring hexane solution. The vessel was placed under vacuum, sealed, and stirred for 24 h. After stirring, the volume was reduced to 2 mL of hexane. Acetonitrile (5 mL) was added, and a brown jellylike solid was formed. The solid was titurated (15 min) until a brown powder formed. The brown solid was filtered, washed with acetonitrile five times, and dried in vacuo (512 mg, 72% yield). ^{1}H NMR (500 MHz, C_6D_6): δ 4.77 (m, 1H), 2.91 (d, 1H), 2.54 (m, 1H), 1.82 (d, 2H), 1.58 (qt, 2H), 1.34 (d, 3H), 1.19 and 1.15 (d of d, 8H), 1.0 (m, 1H). ^{13}C NMR (500 MHz, C_6D_6): δ 88.41, 51.59, 45.49, 35.12, 32.28, 25.87, 23.23, 23.13, 21.59, 16.45. IR (KBr plates, Nujol mull): 1021 cm^{-1} [ν(WN)].

Reaction of $(^tBuO)_3Mo{\equiv}N$ with $W_2(O^tBu)_6$. $W_2(O^tBu)_6$ (0.25 g) and hexanes (10 mL) were added to a Schlenk flask and allowed to stir. Separately $(^tBuO)_3Mo{\equiv}N$ (0.20 g) and hexanes (10 mL) were added to a second Schlenk flask and allowed to stir. The $(^tBuO)_3Mo{\equiv}N$ solution was added to the $W_2(O^tBu)_6$ solution via a cannula. The mixture was left to stir at room temperature overnight. A white precipitate formed, and the solution was filtered. The white solid was identified as $(Bu^tO)_3WN$ by NMR and mass spectrometry. The filtrate was concentrated and yielded a red microcrystalline solid. By mass spectrometry, the ions $Mo_2(OBu^t)_6^+$ and $MoW(OBu^t)_6^+$ were identified.

Reaction of $(^tBuO)_3Cr{\equiv}N$ with $Mo_2(O^tBu)_6$. $(^tBuO)_3Cr{\equiv}N$ (0.057 g, 0.2 mmol) was added with hexanes (10 mL) to a Schlenk flask and allowed to stir. Separately, $Mo_2(O^tBu)_6$ (0.126 g, 0.2 mmol) was added with hexanes (10 mL) to a Schlenk flask and allowed to stir. Both flasks were placed in a dry ice/acetone bath and were allowed to stir for 1 h until the solution had cooled to −78 °C. The $(^tBuO)_3Cr{\equiv}N$ solution was slowly (15 min) added via a cannula to the $Mo_2(O^tBu)_6$ solution. The mixture was kept at −78 °C and was allowed to stir for 2 h. The solvent was removed in vacuo. As the flask slowly warmed, a bluish-green liquid formed around the stopper of the flask. The bluish-green volatile compound was identified as $Cr(O^tBu)_4$ by comparison of the IR spectrum with that of known $Cr(O^tBu)_4$. ^{1}H NMR of the reaction mixture (C_6D_6 solvent, C_6D_5H reference, ppm): δ 1.59 (bs), 1.57 (s), 1.55 (s), 1.48 (s, (^tBuO)$_3$Mo≡N). The mass spectrum of the dried reaction product showed the $(^tBuO)_3Mo{\equiv}N)^+$ ion.

Reaction of $(^tBuO)_3Cr{\equiv}N$ with $W_2(O^tBu)_6$. $(^tBuO)_3Cr{\equiv}N$ (0.063 g, 0.22 mmol) was added with hexanes (10 mL) to a Schlenk flask and allowed to stir. Separately, $W_2(O^tBu)_6$ (0.177 g, 0.22 mmol) was added with hexanes (10 mL) to a Schlenk flask and allowed to stir. Both flasks were placed in a dry ice/acetone bath and were allowed to stir for 1 h until the solutions had cooled to −78 °C. The $(^tBuO)_3Cr{\equiv}N$ solution was slowly (15 min) added via a cannula to the $W_2(O^tBu)_6$ solution. The mixture was kept at −78 °C and was allowed to stir for 2 h. The solvent was removed in vacuo. As the flask slowly warmed, a bluish-green liquid formed around the stopper of the flask. The bluish-green volatile compound was identified as $Cr(O^tBu)_4$ by comparison of the IR spectrum with that of known $Cr(O^tBu)_4$.[31] ^{1}H NMR of the reaction mixture (C_7D_8 solvent, C_7D_7H reference, ppm): δ 3.42 (s), 2.1 (s), 1.59 (s, (^tBuO)$_3$W≡N), 1.48 (s), 1.45 (s). The mass spectrum of the dried reaction product has the correct peak range for $(^tBuO)_3W{\equiv}N$).

Reaction of $(^tBuO)_3W{\equiv}{}^{15}N$ with $(^tBuO)_3Mo{\equiv}N$. $(^tBuO)_3W{\equiv}{}^{15}N$ (0.0209 g, 0.05 mmol) and $(^tBuO)_3Mo{\equiv}N$ (0.0165 g, 0.05 mmol) were added to a NMR tube and allowed to react in THF-d_8

(35) (a) Burke, K.; Perdew, J. P.; Wang, Y. In *Electronic Density Functional Theory: Recent Progress and New Directions*; Dobson,J. F., Vignale, G., Das, M. P., Eds.; Plenum: New York, 1998; pp 81−111. (b) Perdew, J. P. In *Electronic Structure of Solids '91*; Ziesche, P., Eschrig, H., Eds.; Akademie Verlag: Berlin, 1991; p 11. (c) Perdew, J. P.; Chevary, J. A.; Vosko, S. H.; Jackson, K. A.; Pederson, M. R.; Sing, D. J.; Fiolhais, C. *Phys. Rev. B: Condens. Matter* **1992**, *46*, 6671. (d) Perdew, J. P.; Chevary, J. A.; Vosko, S. H.; Jackson, K. A.; Pederson, M. R.; Singh, D. J.; Fiolhais, C. *Phys. Rev. B: Condens. Matter* **1993**, *48*, 4978. (e) Perdew, J. P.; Burke, K.; Wang, Y. *Phys. Rev. B: Condens. Matter* **1996**, *54*, 1653.

(36) (a) Hay, P. J.; Wadt, W. R. *J. Chem. Phys.* **1985**, *82*, 270. (b) Wadt, W. R.; Hay, P. J. *J. Chem. Phys.* **1985**, *82*, 284. (c) Hay, P. J.; Wadt, W. R. *J. Chem. Phys.* **1985**, *82*, 299.

(37) (a) Huzinaga, S. *Gaussian Basis Sets for Molecular Calculations*; Elsevier Science Publishing Co.: Amsterdam, The Netherlands, 1984. (b) Ehlers, A. W.; Bohme, M.; Dapprich, S.; Gobbi, A.; Hollwarth, A.; Jonas, B.; Kohler, K. F.; Stegmann, R.; Veldkamp, A.; Frenking, G. *Chem. Phys. Lett.* **1993**, *208*, 111.

(38) (a) Ditchfield, R.; Hehre, W. J.; Pople, J. A. *J. Chem. Phys.* **1971**, *54*, 724. (b) Hehre, W. J.; Ditchfield, R.; Pople, J. A. *J. Chem. Phys.* **1972**, *56*, 2257. (c) Hariharan, P. C.; Pople, J. A. *Mol. Phys.* **1974**, *27*, 209. (d) Gordon, M. S. *Chem. Phys. Lett.* **1980**, *76*, 163. (e) Hariharan, P. C.; Pople, J. A. *Theor. Chim. Acta* **1973**, *28*, 213.

(39) Andrae, D.; Hauessermann, U.; Dolg, M.; Preuss, H. *Theor. Chim. Acta* **1990**, *77*, 123.

(40) Dunning, T. H., Jr. *J. Chem. Phys.* **1989**, *90*, 1007.

(41) (a) Fukui, K. *J. Phys. Chem.* **1970**, *74*, 4161. (b) Fukui, K. *Acc. Chem. Res.* **1981**, *14*, 363.

at room temperature for 1 week. The ^{1}H NMR spectrum of the reaction mixture shows no change from the starting materials. The ^{15}N NMR spectrum of the reaction mixture (THF-d_8 solvent, THF-d_7 reference, ppm): δ 828.8 (s, (^{t}BuO)$_3$Mo≡^{15}*N*), 731.8 (^{t}BuO)$_3$W≡^{15}*N*). Mass spectral analysis of the reaction products verifies the presence of (^{t}BuO)$_3$Mo≡^{15}N.

Reaction of (^{t}BuO)$_3$W≡CMe with (^{t}BuO)$_3$Mo≡N. (^{t}BuO)$_3$W≡CMe (0.0215 g, 0.05 mmol) was made in an NMR tube according to a previously reported method. (^{t}BuO)$_3$Mo≡N (0.0165 g, 0.05 mmol) was added to the tube and allowed to react at room temperature for 1 week. ^{1}H NMR of the reaction mixture (C_6D_6 solvent, C_6D_5H reference, ppm): δ 3.57 (s, 3H, J_{HW} = 7.2 Hz, (^{t}BuO)$_3$W≡C*Me*), 2.58 (s, 3H, (^{t}BuO)$_3$Mo≡C*Me*), 1.48 (s, 27H, (^{t}*Bu*O)$_3$Mo≡N), 1.46 (s), 1.44 (s, 27H, (^{t}*Bu*O)$_3$W≡CMe), 1.44 (s), 1.42 (s). ^{13}C{^{1}H} NMR (C_6D_6 solvent, C_6D_5H reference, ppm): δ 333.1 (s), 279.6 (s, 1H, (^{t}BuO)$_3$Mo≡*C*Me), 254.1 (s, 1H, J_{CW} = 306.5 Hz, (^{t}BuO)$_3$W≡*C*Me).

Reaction of (^{t}BuO)$_3$W≡CMe with (^{t}BuO)$_3$Mo≡CPh. (^{t}BuO)$_3$W≡CMe (0.0054 g, 0.0125 mmol) was made in an NMR tube according to a previously reported method. (^{t}BuO)$_3$Mo≡CPh (0.0051 g, 0.0125 mmol) was added to the tube and allowed to react at room temperature for 1 week. ^{1}H NMR of the reaction mixture (C_6D_6 solvent, C_6D_5H reference, ppm): δ 7.49 (d, 2H, (^{t}BuO)$_3$Mo≡C*Ph*), 7.33 (d, 2H, (^{t}BuO)$_3$W≡C*Ph*), 7.23 (t, 2H, (^{t}BuO)$_3$W≡C*Ph*), 7.09 (t, 2H, (^{t}BuO)$_3$Mo≡C*Ph*), 6.87 (t, 1H, (^{t}BuO)$_3$Mo≡C*Ph*), 6.82 (t, 1H, (^{t}BuO)$_3$W≡C*Ph*), 3.57 (s, 3H, J_{HW} = 7.2 Hz, (^{t}BuO)$_3$W≡*C*Me), 2.58 (s, 3H, (^{t}BuO)$_3$Mo≡C*Me*), 1.49 (s, 27H, (^{t}*Bu*O)$_3$Mo≡CPh), 1.48 (s), 1.44 (s, 27H, (^{t}*Bu*O)$_3$W≡CMe), 1.42 (s, 27H, (^{t}*Bu*O)$_3$W≡CPh). ^{13}C{^{1}H} NMR of reaction mixture (C_6D_6 solvent, C_6D_5H reference, ppm): δ 333.1 (s), 307.8 (s), 279.8 (s, 1H, (^{t}BuO)$_3$Mo≡*C*Ph), 254.1 (s, 1H, J_{CW} = 306.5 Hz, (^{t}BuO)$_3$W≡*C*Me).

Reaction of (^{t}BuO)$_3$W≡C^{i}Pr with (^{t}BuO)$_3$Mo≡N. (^{t}BuO)$_3$W≡C^{i}Pr (0.0229 g, 0.05 mmol) and (^{t}BuO)$_3$Mo≡N (0.0165 g, 0.05 mmol) were added to a NMR tube and allowed to react at room temperature for 1 week. ^{1}H NMR of reaction mixture (C_6D_6 solvent, C_6D_5H reference, ppm): δ 4.05 (sept, 1H, J_{HW} = 6.85 Hz, (^{t}BuO)$_3$W≡C^i*Pr*), 3.11 (sept, 1H, (^{t}BuO)$_3$Mo≡C^i*Pr*), 1.48 (s, 27H, (^{t}*Bu*O)$_3$Mo≡N), 1.47 (s, 27H, (^{t}*Bu*O)$_3$Mo≡C^{i}Pr), 1.46 (s, 27H, (^{t}*Bu*O)$_3$W≡C^{i}Pr), 1.45 (s, 27H, (^{t}*Bu*O)$_3$W≡N), 1.24 (d, 6H, (^{t}BuO)$_3$W≡C^i*Pr*), 1.16 (d, 6, (^{t}BuO)$_3$Mo≡C^i*Pr*).

Preparation of Samples for the Determination of Kinetics. All samples were prepared in an NMR tube equipped with a J. Young adapter. For all runs, a stock solution of Me^{13}CN in THF-d_8 was prepared by weighing 48.5 mg in a 5 mL volumetric flask to produce a 0.231 M solution. For determination of the enthalpy parameters, 890 μL of THF-d_8 was added to 11.3 mg of (^{t}BuO)$_3$W^{15}N via a gastight syringe and transferred to the NMR tube. Addition of 110 μL of the stock solution with a gastight syringe followed. Preparation occurred immediately before NMR spectra were collected. In this instance, the catalyst and nitrile concentrations remained constant throughout the temperature range (50, 40, 35, and 21 °C). In each case, the sample was heated in the probe, and once the overnight run finished, the sample was removed and placed in its respective temperature oil bath for the time. In the case of the determination of the reaction order in nitrile, the amount of catalyst remained the same, while the amount of stock solution was changed according to the desired ratio (cat:nitrile = 1:1, 1:0.5, 1:2).

The nitrile cleavage reaction involving Me^{13}CN was monitored by ^{13}C{^{1}H} NMR spectroscopy. The parameters used were as follows: number of scans (NS = 15), number of data points (TD = 65 536), receiver gain (RG = 2896), and relaxation time (D1 = 75 s). The deconvolution of ^{13}C NMR spectra was done using XWIN-NMR version 3.5 PL6. The T_1 relaxation times for acetonitrile (15.2 s) ^{13}C NMR signals were measured at 298 K. The Ernst equation (1) (where $t_1 = T_1$ relaxation time, pw 90 = 90° pulse width, at = acquistion time, and d1 = delay time between pulses). NMR probe temperatures were calibrated with a sample of ethylene glycol, and van Greet's equation was used to determine the optimal pulse widths for the delay time used in NMR experiments.

Calculation of the Kinetics and Activation Parameters. The absolute concentration of the catalyst in solution was determined by a proton integration of the O^{t}Bu resonance (s, 1.49 ppm) versus the Me^{13}C≡N methyl resonance (d, 1.95 J= 10.7 Hz). The cleavage and atom exchange was measured by following the disappearance of a singlet at 115.9 ppm (Me^{13}*C*≡N) and the appearance of a doublet at 115.95 and 115.82 ppm (Me^{13}*C*≡^{15}N). The Lorentzian deconvolution of ^{13}C NMR spectra was performed using XWIN-NMR 3.5 PL6. All of the cleavage and atom exchange reactions were of the type A + B ↔ C + D, where the rate law was determined (eq 2) and where $\Delta = [A] - [A]_{eq}$.

When $\ln[(\Delta/(\Delta(1 - 1/K) + [A]_e + [B]_e + (1/K)([C]_e + [D]_e))]$ is plotted versus time, the slope is inserted into eq 2 to solve for k_{obs}. The enthalpy parameters were calculated by plotting $\ln(k_{obs}/T)$ versus $1/T$, where the slope $= -\Delta H^{\ddagger}/R$ and the intercept $= \Delta S^{\ddagger}/R + 23.8$.

Acknowledgment. We thank the National Science Foundation for financial support and gratefully acknowledge the Ohio Supercomputer Center for computational resources.

Supporting Information Available: Free energy (at 298 K) profiles for a N-atom exchange reaction between (MeO)$_3$M≡N (where M = W, Mo) and MeC≡N and structures of transition states and intermediates with selected calculated structural parameters calculated based on BS-II (Figures S1 and S2). This material is available free of charge via the Internet at http://pubs.acs.org.

IC8003917